U.S. National Library of Medicine
National Center for Biotechnology Information

NLM Citation: The MICAD Research Team. ^{76}Br-Human recombinant anti-ED-B fibronectin L19-small immunoprotein. 2007 Aug 4 [Updated 2007 Aug 27]. In: Molecular Imaging and Contrast Agent Database (MICAD) [Internet]. Bethesda (MD): National Center for Biotechnology Information (US); 2004-2013.
Bookshelf URL: https://www.ncbi.nlm.nih.gov/books/

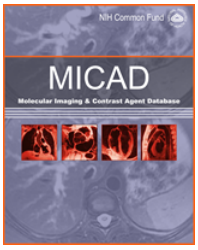

^{76}Br-Human recombinant anti-ED-B fibronectin L19-small immunoprotein

^{76}Br-L19-SIP

The MICAD Research Team

Created: August 4, 2007; Updated: August 27, 2007.

Chemical name:	^{76}Br-Human recombinant anti-ED-B fibronectin L19-small immunoprotein	
Abbreviated name:	^{76}Br-L19-SIP	
Synonym:	^{76}Br-ED-B fibronectin-binding human antibody derivative	
Agent Category:	Small immunoprotein (SIP)	
Target:	ED-B Fibronectin (ED-B FN)	
Target Category:	Antibody-antigen binding	
Method of detection:	Positron emission tomography (PET)	
Source of signal:	^{76}Br	
Activation:	No	
Studies:	• *In vitro* • Rodents	Click on protein, nucleotide (RefSeq), and gene for more information about ED-B fibronectin.

Background

[PubMed]

The ^{76}Br-human recombinant anti-ED-B fibronectin L19-small immunoprotein (^{76}Br-L19-SIP) is a radiolabeled molecular imaging agent developed for positron emission tomography (PET) imaging of tumor angiogenesis and guidance for antiangiogenic treatment (1). ^{76}Br is a positron emitter with a 54% abundance and a half-life ($t_{½}$) of 16.2 h.

Angiogenesis is a process of development and growth of new blood vessels from pre-existing vessels (2). Tumor growth depends on the formation of new blood vessels from this process. Normal angiogenesis is orderly and highly regulated, whereas tumor angiogenesis is chaotic and irregular. Abnormal angiogenesis is important in the carcinogenesis, growth, and progression of solid and hematologic tumors in humans (3). Fibronectins (FNs) are a family of universal cell-adhesion molecules that are widely distributed (4). FN is a polymorphic glycoprotein of ~2,500 amino acids and has a high molecular mass of 250–280 kDa. FN occurs in soluble form in plasma and other body fluids and in insoluble form in the extracellular matrices (5, 6). Both forms are dimers composed of a series of repeating units of three types and joined by two disulfide bonds at the C-terminus of the molecule. FN polymorphism arises from alternative splicing patterns of the pre-mRNA or post-translational

modifications of FN itself (6). The splice variant ED-B FN is highly expressed during angiogenesis in both neoplastic and normal tissues (7), but higher levels of ED-B expression have been found in primary and metastatic tumors in breast, colorectal, and non-small cell lung cancers (4, 8-10).

Molecular imaging of angiogenesis offers serial non-invasive evaluation of both location and growth dynamics of tumors (11). PET or single-photon emission computed tomography imaging with an appropriate radiolabeled tracer targeted to angiogenic pathways may allow the evaluation of specific aspects of tumor vascular biology (10). A molecular probe that targets ED-B FN can be both an early tumor marker and a tool to monitor the success of antiangiogenic cancer therapy. The human recombinant single-chain antibody fragment (scFv) L19, which has a high affinity for ED-B FN, was developed by Pini et al. (12). Borsi et al (13). used the variable regions of L19 to construct a bivalent human SIP by fusing two scFvs to the ϵCH_4 domain of the secretory isoform S2 of human IgE ($\epsilon_{s2}-CH_4$). The $\epsilon_{s2}-CH_4$ domain provides a covalent stabilization of the dimer (molecular mass = ~80 kDa) (14). This group of researchers and Tijink et al (15) prepared radioiodinated L19-SIP that showed specific accumulation around tumor neovasculature and tumor stroma with high ED-B expression. In an effort to develop a PET molecular probe, Rossin et al. (1) used enzymatic radiobromination to prepare ^{76}Br-L19-SIP and performed biodistribution and PET imaging studies in mice bearing the mouse embryonal teratocarcinoma F9. ^{76}Br has relatively favorable production and photon yieldsand ^{76}Br has a sufficiently long physical $t_{½}$ for PET imaging up to 48 h after injection.

Synthesis

[PubMed]

Pini et al. (12) constructed and used a large synthetic phage-display human antibody library (>3 × 10^8 clones) to produce L19 with a very high affinity (dissociation constant (K_d) = 54 pM) for the ED-B domain of FN. L19 was cloned in scFv configuration in the novel phagemid vector pDN332. Borsi et al. (13) reported the construction of the L19-SIP gene by DNA sequence amplification and insertion into the pUT-ϵSIP vector. The L19-scFv was connected to the $\epsilon_{s2}-CH_4$ domain by a short GGSG linker. The SIP gene was cloned into the mammalian expression vector pcDNA3 to obtain the construct pcDNA3-L19-SIP. This construct was used to transfect SP2/0 murine myeloma cells for expression. Immunoaffinity chromatography was used to purify the collected L19-SIP. Rossin et al. (1) prepared ^{76}Br-L19-SIP based on a modified enzymatic method of Lovqvist et al. (16). Briefly, ^{76}Br-labeled bromide was produced by the ^{76}Se(p,n)^{76}Br nuclear reaction on a ^{76}Se-enriched Cu_2Se target and recovered by dry distillation. L19-SIP was mixed with ^{76}Br-labeled bromide and 0.6 U bromoperoxidase in 300 µl 50 mmol/L phosphate buffer (pH 7.0) containing 80 µmol/L hydrogen peroxide. The reaction mixture was incubated at 0°C for 80 min. When <37 MBq (1 mCi) ^{76}Br was used, the radiolabeling yield was 82 ± 2% (n = 4). For >37 MBq (1 mCi) ^{76}Br, the radiochemical yield was 55% (n = 2). Analysis with radio-fast-protein liquid chromatography (radio-FPLC) showed that the ^{76}Br-L19-SIP used for animal experiments had a radiochemical purity >90%. The specific activity was not reported, but the dose for the animal biodistribution studies was ~185 kBq/µg (5 µCi/µg) or ~14.8 kBq/pmol (0.4 µCi/pmol) based on the molecular mass of ~80 kDa, and the dose for the imaging study was ~440 kBq/µg (11.89 µCi/µg) or 35.2 kBq/pmol (0.95 µCi/pmol).

In Vitro Studies: Testing in Cells and Tissues

[PubMed]

Rossin et al. (1) determined the *in vitro* immunoreactivity of ^{76}Br-L19-SIP to be 80 ± 2% (n = 5) by affinity chromatography. The *in vitro* stability of ^{76}Br-L19-SIP was studied by incubating the radioligand in mouse serum at 37°C. After 48 h incubation, radio-FPLC analysis detected no free ^{76}Br-labeled bromide, but 21% of the yield comprised of high molecular weight impurities.

Animal Studies

Rodents

[PubMed]

Biodistribution studies (n = 3–4) of ^{76}Br-L19-SIP were performed in mice bearing subcutaneous mouse embryonal teratocarcinoma F9 tumors (0.1–2.8 g) (1). F9 tumors were previously reported to express high levels of ED-B FN (13). Each mouse received ~1.3 MBq (35 μCi) ^{76}Br-L19-SIP (~185 kBq/μg or 5 μCi/μg) or ~0.35 mg antibody/kg body weight by i.v. administration. ^{76}Br-L19-SIP showed high radioactivity localization in the tumor but slow clearance from the blood and blood-rich organs. The tumor radioactivity levels of ^{76}Br-L19-SIP, expressed as percentage of injected dose per gram (% ID/g), were 18.1 ± 7.6 (5 h), 9.3 ± 3.5 (24 h), and 14.3 ± 1.6 (48 h). The tumor/blood ratios were 0.8 ± 0.4 (5 h), 1.2 ± 0.5 (24 h), and 1.8 ± 0.4 (48 h). The tumor/muscle ratios were 7.3 ± 3.1 (5 h), 2.3 ± 1.1 (24 h), and 5.6 ± 0.6 (48 h). There were also high radioactivity levels in the mouse reproductive organs (uterus and ovaries), which express the ED-B fibronectin. At 5 h, the radioactivity levels (% ID/g) in other major organs were 7.0 ± 2.3 (ovaries), 22.4 ± 3.7 (blood), 11.4 ± 2.0 (lung), 5.0 ± 0.3 (liver), 5.7 ± 0.6 (spleen), 5.5 ± 2.5 (thyroid), 13.5 ± 6.3 (uterus), 9.4 ± 1.9 (kidney), 6.2 ± 0.6 (heart), 2.5 ± 0.2 (muscle), and 3.6 ± 0.6 (bone). By 48 h, these radioactivity levels (% ID/g) decreased to 1.8 ± 0.3 (ovaries), 8.1 ± 1.7 (blood), 5.8 ± 0.9 (lung), 2.5 ± 0.5 (liver), 2.9 ± 0.7 (spleen), 2.4 ± 0.3 (thyroid), 6.0 ± 1.0 (uterus), 4.1 ± 1.2 (kidney), 2.7 ± 0.5 (heart), 2.6 ± 0.0 (muscle), and 2.6 ± 0.4 (bone). Renal elimination was slow with only 4.7 ± 0.9% ID at 48 h. No specific blocking study was performed.

Metabolic studies of ^{76}Br-L19-SIP were conducted in normal mice (n = 3) (1). Each mouse received ~1.8 MBq (48.65 μCi) ^{76}Br-L19-SIP (~0.2 mg/kg body weight) by i.v. administration. In the serum, radio-FPLC analysis showed that the amounts of intact ^{76}Br-L19-SIP were 86.1 ± 1.7%, 73.5 ± 0.5%, and 24.7 ± 0.9% at 2 h, 5 h, and 24 h after injection, respectively. The immunoreactivity of these samples were 65%, 66%, and 21%, respectively. In the urine, the majority of the radioactivity was ^{76}Br-labeled bromide. The amounts of intact ^{76}Br-L19-SIP were 7.7 ± 0.1%, 5.8 ± 0.6%, and 0.8 ± 0.3% at 2 h, 5 h, and 24 h, respectively, in urine.

PET imaging was performed in mice (n = 4) bearing subcutaneous F9 tumors (0.1–2.8 g) (4). Each mouse was injected with ~13 MBq (351 μCi) ^{76}Br-L19-SIP (~440 kBq/μg or 11.89 μCi/μg) by i.v. administration. Microcomputed tomography imaging studies were also performed for landmark registration. Imaging with ^{76}Br-L19-SIP produced clear tumor images at 5, 24, and 48 h. The radioactivity distribution pattern was similar to the biodistribution studies. The background radioactivity in the abdominal area was high. The kidneys, heart, and aorta were visualized at earlier time points. The stomach and bladder were visualized at 48 h. The tumor standard uptake values (radioactivity concentration in μCi/ml divided by the injected dose in μCi/animal weight in g) obtained by semiquantitative analysis of microPET images were 2.4 ± 0.5 (5 h), 2.7 ± 0.1 (24 h), and 2.4 ± 0.2 (48 h).

Other Non-Primate Mammals

[PubMed]

No publication is currently available.

Non-Human Primates

[PubMed]

No publication is currently available.

Human Studies

[PubMed]

No publication is currently available.

References

1. Rossin R., Berndorff D., Friebe M., Dinkelborg L.M., Welch M.J. Small-animal PET of tumor angiogenesis using a (76)Br-labeled human recombinant antibody fragment to the ED-B domain of fibronectin. J Nucl Med. 2007; **48** (7):1172–9. PubMed PMID: 17574989.
2. Shinkaruk S., Bayle M., Lain G., Deleris G. Vascular endothelial cell growth factor (VEGF), an emerging target for cancer chemotherapy. Curr Med Chem Anticancer Agents. 2003; **3** (2):95–117. PubMed PMID: 12678905.
3. Ranieri G., Patruno R., Ruggieri E., Montemurro S., Valerio P., Ribatti D. Vascular endothelial growth factor (VEGF) as a target of bevacizumab in cancer: from the biology to the clinic. Curr Med Chem. 2006; **13** (16):1845–57. PubMed PMID: 16842197.
4. Berndorff D., Borkowski S., Moosmayer D., Viti F., Muller-Tiemann B., Sieger S., Friebe M., Hilger C.S., Zardi L., Neri D., Dinkelborg L.M. Imaging of tumor angiogenesis using 99mTc-labeled human recombinant anti-ED-B fibronectin antibody fragments. J Nucl Med. 2006; **47** (10):1707–16. PubMed PMID: 17015908.
5. Carnemolla B., Balza E., Siri A., Zardi L., Nicotra M.R., Bigotti A., Natali P.G. A tumor-associated fibronectin isoform generated by alternative splicing of messenger RNA precursors. J Cell Biol. 1989; **108** (3):1139–48. PubMed PMID: 2646306.
6. Kosmehl H., Berndt A., Katenkamp D. Molecular variants of fibronectin and laminin: structure, physiological occurrence and histopathological aspects. Virchows Arch. 1996; **429** (6):311–22. PubMed PMID: 8982375.
7. Castellani P., Viale G., Dorcaratto A., Nicolo G., Kaczmarek J., Querze G., Zardi L. The fibronectin isoform containing the ED-B oncofetal domain: a marker of angiogenesis. Int J Cancer. 1994; **59** (5):612–8. PubMed PMID: 7525495.
8. Kaczmarek J., Castellani P., Nicolo G., Spina B., Allemanni G., Zardi L. Distribution of oncofetal fibronectin isoforms in normal, hyperplastic and neoplastic human breast tissues. Int J Cancer. 1994; **59** (1):11–6. PubMed PMID: 7927891.
9. Pujuguet P., Hammann A., Moutet M., Samuel J.L., Martin F., Martin M. Expression of fibronectin ED-A+ and ED-B+ isoforms by human and experimental colorectal cancer. Contribution of cancer cells and tumor-associated myofibroblasts. Am J Pathol. 1996; **148** (2):579–92. PubMed PMID: 8579120.
10. Santimaria M., Moscatelli G., Viale G.L., Giovannoni L., Neri G., Viti F., Leprini A., Borsi L., Castellani P., Zardi L., Neri D., Riva P. Immunoscintigraphic detection of the ED-B domain of fibronectin, a marker of angiogenesis, in patients with cancer. Clin Cancer Res. 2003; **9** (2):571–9. PubMed PMID: 12576420.
11. Laking, G.R. and P.M. Price, Positron emission tomographic imaging of angiogenesis and vascular function. Br J Radiol, 2003. 76 Spec No 1: p. S50-9.
12. Pini A., Viti F., Santucci A., Carnemolla B., Zardi L., Neri P., Neri D. Design and use of a phage display library. Human antibodies with subnanomolar affinity against a marker of angiogenesis eluted from a two-dimensional gel. J Biol Chem. 1998; **273** (34):21769–76. PubMed PMID: 9705314.
13. Borsi L., Balza E., Bestagno M., Castellani P., Carnemolla B., Biro A., Leprini A., Sepulveda J., Burrone O., Neri D., Zardi L. Selective targeting of tumoral vasculature: comparison of different formats of an antibody (L19) to the ED-B domain of fibronectin. Int J Cancer. 2002; **102** (1):75–85. PubMed PMID: 12353237.
14. El-Emir E., Dearling J.L., Huhalov A., Robson M.P., Boxer G., Neri D., van Dongen G.A., Trachsel E., Begent R.H., Pedley R.B. Characterisation and radioimmunotherapy of L19-SIP, an anti-angiogenic antibody

against the extra domain B of fibronectin, in colorectal tumour models. Br J Cancer. 2007; **96** (12):1862–70. PubMed PMID: 17519905.

15. Tijink B.M., Neri D., Leemans C.R., Budde M., Dinkelborg L.M., Stigter-van Walsum M., Zardi L., van Dongen G.A. Radioimmunotherapy of head and neck cancer xenografts using 131I-labeled antibody L19-SIP for selective targeting of tumor vasculature. J Nucl Med. 2006; **47** (7):1127–35. PubMed PMID: 16818947.
16. Lovqvist A., Sundin A., Ahlstrom H., Carlsson J., Lundqvist H. Pharmacokinetics and experimental PET imaging of a bromine-76-labeled monoclonal anti-CEA antibody. J Nucl Med. 1997; **38** (3):395–401. PubMed PMID: 9074527.